Please cite the Published Version

Additional Information: This is an open access article which first appeared in ChemPhysChem

Data Access Statement: The data that support the findings of this study are available from the corresponding author upon reasonable request.

ChemPhysChem

Research Article
doi.org/10.1002/cphc.202200216

Chemistry Europe
European Chemical
Societies Publishing

www.chemphyschem.org

Molecular Dynamics Simulations of Nitric Oxide Scattering Off Graphene

Thomas Greenwood*[a] and Sven P. K. Koehler[a, b]

We performed classical molecular dynamics simulations to model the scattering process of nitric oxide, NO, off graphene supported on gold. This is motivated by our desire to probe the energy transfer in collisions with graphene. Since many of these collision systems comprising of graphene and small molecules have been shown to scatter non-reactively, classical molecular dynamics appear to describe such systems sufficiently. We directed thousands of trajectories of NO molecules onto graphene along the surface normal, while varying impact position, but also speed, orientation, and rotational excitation of the nitric oxide, and compare the results with experimental data. While experiment and theory do not match quantitatively, we observe agreement that the relative amount of kinetic energy lost during the collision increases with increasing initial kinetic energy of the NO. Furthermore, while at higher collision energies, all NO molecules lose some energy, and the vast majority of NO is scattered back, in contrast at low impact energies, the fraction of those nitric oxide molecules that are trapped at the surface increases, and some NO molecules even gain some kinetic energy during the collision process. The collision energy seems to preferentially go into the collective motion of the carbon atoms in the graphene sheet.

Introduction

Molecular dynamics (MD) simulations are a useful way to model both static molecular structures,[1,2] but also non-reactive (chemical) processes such as adsorption and desorption phenomena.[3,4] Classical MD simulations are based on force fields and do not explicitly include contributions from electrons,[5] and as such in their simplest form cannot model chemical reactions.[6,7] They also lack the precision of *ab initio* methods,[8] and naturally cannot model quantum effects. However, due to the reduced computational cost compared to quantum methods, MD simulations allow processes over much longer timescales to be modelled, and hence can help to catch a glimpse of such processes in a fashion not too dissimilar to a molecular movie.

We have recently investigated experimentally the scattering of nitric oxide, NO, off graphene.[9] This was in part motivated by the fact that NO is a diatomic radical, hence potentially reactive with graphene, but NO also allows rotational distributions to be observed, unlike monoatomic radicals. However, the by far largest contribution of scattered NO is due to *direct inelastic* scattering, and this is a process that can conveniently

be modelled using MD simulations, allowing us to create snapshots of the actual scattering process. We have hence performed MD simulations of NO directed with various speeds at normal incidence angle at graphene supported by 6 layers of gold. This allows us to derive speed and angular distribution of the scattered NO for comparison with experimental results. The experiment also delivers rotational energy distributions of NO, and we also derived these classically in the simulations presented here. Furthermore, the MD simulations allow us to extract properties that are currently not accessible in our experiments such as the range of heights of the NO above the graphene at the turning point, i.e. when it is closest to the graphene surface, and the effect of varying conditions such as the initial velocity, which will guide us in future experiments.

The scattering of hydrogen off graphene has already been investigated both experimentally and theoretically.[10–12] The scattering of atoms other than hydrogen (N(^{4}S) and O(^{3}P), respectively) with graphene has also been modelled by Nieman *et al.* and Jayee *et al.*;[13,14] quantum-methods guaranteed that chemical reactions with the graphene (insertion) and ablation reactions could be observed.

Both classical mechanics as well as *ab initio* molecular dynamics simulations were also employed in modelling the collisions of homo-diatomic molecules (N_2 and O_2) with highly oriented pyrolytic graphite (HOPG),[15–17] in which direct scattering has been found to be the dominant process, but some evidence for trapping-desorption was observed, too. The fact that MD simulations allow for larger entities (many more atoms) to be modelled allowed Hase and co-workers to observe that most of the initial kinetic energy is channelled into the surface motions of the graphene substrate.[15–17]

Collisions of NO with graphite were also experimentally and theoretically investigated from the 1980s onwards. Nyman *et al.* modelled the scattering process classically and in a statistical fashion;[18,19] they observed 'rotational cooling' (at surface

[a] T. Greenwood, Prof. Dr. S. P. K. Koehler
     Department of Natural Sciences
     Manchester Metropolitan University
     M1 5GD, Manchester, UK
     E-mail: thomas.greenwood@stu.mmu.ac.uk
[b] Prof. Dr. S. P. K. Koehler
     Fakultät II, Hochschule Hannover
     Ricklinger Stadtweg 120, 30459 Hannover, Germany
     Homepage: http://www.koehler.wp.hs-hannover.de

temperatures of 300 K or higher) and even rotational rainbows. Many more studies investigated the NO-graphite system experimentally by measuring in particular speed and angular distributions as well as rotational state distributions.[20,21] Specular scattering is almost always observed, especially at higher temperatures, and an isotropic component, presumably due to a trapping desorption mechanism, becomes dominant at lower temperatures,[22,23] even at fairly steep incidence angles.[24]

We here set out to perform simulations of the scattering of NO radicals off graphene supported on gold using classical MD methods, i.e. without considering quantum effects. We replicate the conditions in our own experiment, with the aim in particular to establish translational energy and rotational state distributions.

Results and Discussion

Figure 1 shows the speed distributions of NO molecules after collision with a graphene layer supported on gold for initial NO velocities of 600, 800, 1200, 1600 and 2500 m s^{-1} (0.06, 0.10, 0.22, 0.40 and 0.97 eV) from dark-red to orange; the initial velocities are indicated by short vertical arrows at the top, while the horizontal arrows illustrate the difference of speed between the initial speed and the most probable final speed. We only plotted in Figure 1 the case of no rotational excitation, N-atom oriented towards the surface, with a surface temperature equilibrated at 300 K. All data (data points as open circles) are fitted to the 3D flux distribution in equation 1

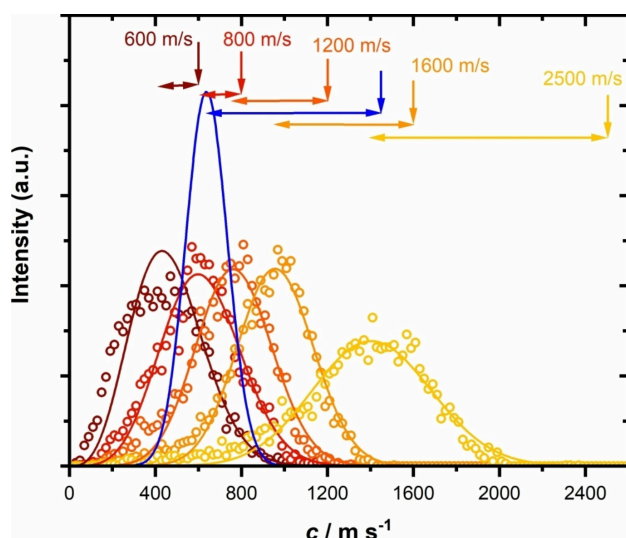$$F(c)dc = A\,c^3\,\exp\frac{-(c-c_0)^2}{\alpha^2}\,dc \qquad (1)$$

Figure 1. Speed distributions of NO molecules after scattering off a graphene surface, initial speeds as indicated by vertical arrows. Horizontal double-arrows indicate the loss of speed, and the blue data is an experimental speed distribution with an initial NO velocity of 1418 m/s and a width of ~190 m/s. All simulation data fitted to eq. 5.

where A is a scaling factor and α is related to the width of the distribution.[25] The blue curve is a fit to an experimental speed distribution with an initial NO velocity of 1418 m/s and a full width at half maximum of ~190 m s^{-1}. A few observations can be made straight away: 1) The faster the incoming NO molecule, the more kinetic energy is transferred (most likely to the graphene surface motions); 2) while for the fastest speeds, all NO molecules are scattered with speeds that are *slower* than the incoming NO, for the slower incoming projectiles, a significant portion actually gains some kinetic energy in the scattering process; 3) while the experimental data is qualitatively similar, it appears as if more kinetic energy is lost during the scattering process in the experiment than predicted in the MD simulations, and interestingly that the speed distribution is *narrower* in the experiment than in the simulations, despite the initial width of the speeds distribution in the experiment being *significantly wider* than in the simulations (where no spread is assumed). This wider speed distribution of the scattered NO molecules in the simulations, however, might be a direct result of the classical rather than quantum nature of the simulations. Naturally, vibrational energy is quantised, but in our simulations, energy exchange of fractions of vibrational quanta are allowed, thus an incoming NO molecule might lose or gain small amounts of energy from e.g. vibrations in the substrate that would not be allowed had a rigorous quantum-mechanical treatment be applied. This possibly leads to the wider velocity distribution in the simulations, but quantum corrections of the classical simulations could solve this issue.[26] The loss of a significant amount of energy for the higher incoming velocities contrasts with previous simulations of scattering on graphene,[12] but this loss is expected due to the different masses of the incoming projectiles, and furthermore it is not straightforward to compare those two experiments due to the different incidence angles. The NO in our simulations is travelling along the surface normal, resulting in more energy being transferred into the surface, whereas the scattering simulations were performed at angles that are removed from the surface normal and as such show less energy transfer as kinetic energy in the surface plane tends to be conserved.[15,16] Scattering simulations of atomic nitrogen with pristine graphene at kinetic energies of 14.9 kcal/mol (0.646 eV) found an energy loss ratio of roughly 0.6,[13] this could again be due to the scattering angle of the nitrogen, or in this case due to a monoatomic particles (N atoms) being scattered rather than a diatomic NO. Nevertheless, the results show that even at this relatively high initial kinetic energy, there is little evidence for reactions such as insertion reactions into pristine graphene.

Research by Hase *et al.* demonstrates how at similar velocities to this study, the vast majority of the initial energy is transferred into surface vibrations and kinetic energy of the scattered N$_2$, again showing that the higher the incident angle (with respect to the surface normal), the less energy is transferred to the surface due to the velocity component along the surface being conserved.[16]

The initial and final speeds and kinetic energies (and energy loss and ratio) for the present molecular dynamics simulations are shown in Table 1:

ChemPhysChem

Research Article
doi.org/10.1002/cphc.202200216

Chemistry Europe
European Chemical
Societies Publishing

Table 1. Initial and most probable final speeds (in $m\,s^{-1}$) and kinetic energies (in eV) and energy loss and ratio. The data for 600, 800, 1200, 1600 and 2500 $m\,s^{-1}$ are from the simulations while the data for 1418 $m\,s^{-1}$ are from experimental work.

$c_i/m\,s^{-1}$	$c_{f,max}$ [$m\,s^{-1}$]	E_i [eV]	$E_{f,max}$ [eV]	ΔE [eV]	E_f/E_i
600	440	0.06	0.03	0.03	0.5
800	606	0.10	0.06	0.04	0.6
1200	755	0.22	0.09	0.13	0.4
1418 ± 95	621 ± 115	0.31 ± 0.08	0.06 ± 0.04	0.25 ± 0.09	0.2 ± 0.1
1600	949	0.40	0.14	0.26	0.3
2500	1384	0.97	0.30	0.67	0.3

Impact angles in all simulations and the experiment are along the surface normal, and if the Baule model in its simplest form was applied, the NO would not scatter off the surface at all as it is heavier than a single C atom. Instead, it appears that in order of increasing speed of the incoming molecules, the NO interacts with a pseudo-atom with a mass of 15, 20, 12, 11, 10 C atoms (for $c_i = 600, 800, 1200, 1600, 2500\,m\,s^{-1}$), and with a pseudo-atom with a mass of ~7 C atoms if the experimental results are used. This means firstly that fewer atoms in the carbon lattice 'work together' or are involved in the scattering process the faster the incoming projectiles are flying (at least for velocities of 800 $m\,s^{-1}$ or greater), and secondly that the 'real' 2D graphene network seems more rigid than described in the MD simulations, leading to the lowest 'effective mass' of a surface atom in the experiments. The reason for the only qualitative rather than quantitative agreement is most likely due to the fact that while the graphene and gold potentials in literature are well-established, the universal force fields used for the interactions between the incoming NO and the graphene and gold were developed for a large range of chemical systems and are hence necessarily a compromise. Ab initio calculations would have likely yielded better potentials and thus a more quantitative agreement with experiment.

Just as the simulations underestimate how much kinetic energy is lost in the collision process, they seem to overestimate the polar angle distribution, see Figure 2. The angular distributions become narrower with increasing initial NO speed as expected, but this increase is not overly pronounced. When fitting the angular distributions to a $\cos^n\theta$ function (where a fitting factor of $n=1$ would indicate a thermal desorption process), the fitting parameter n only increases from 40 to 51 as the initial NO speed increases. All those parameters are a lot smaller than $n=745$ for the experimental data, which remarkably shows the narrowest angular distribution by far, though $\cos^n\theta$ functions with $n>40$ are already fairly narrow, and the much larger fitting parameter n for the experimental work perhaps overstates that the width of the distribution only changes from a rather narrow $\pm 10°$ (simulations) to approximately $\pm 3°$ (experiment). Both simulation data and experimental data include rotational excitation of the incoming NO, but differences in the exact rotational temperature could lead to (slightly) different angular distributions. However, it seems that the graphene surface appears even 'flatter' towards incoming NO molecules than the simulations can reproduce. The narrow scattering distributions at higher incoming velocities match similar studies of H atom scattering off graphene at similar
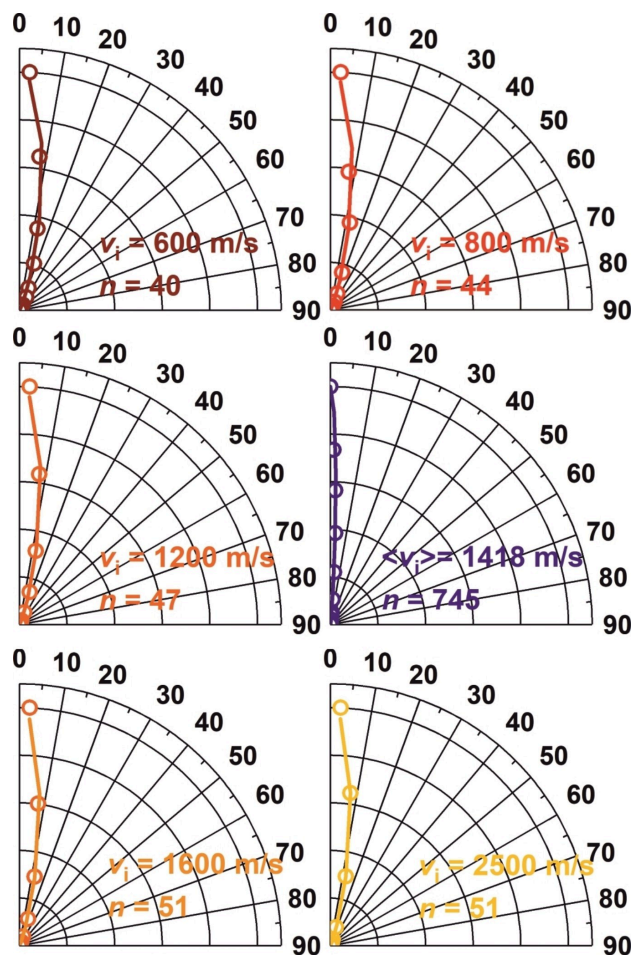
Figure 2. Polar angular distributions of NO molecules after scattering off a 300 K graphene surface, initial speeds as indicated. Blue data is an experimental angular distribution with an initial NO velocity of 1418 $m\,s^{-1}$, and a width of ~190 $m\,s^{-1}$. All data fitted to a $\cos^n\theta$ function, with the fitting parameter n indicated.

kinetic energies (1 eV) with scattering distributions close to the specular angle.[12] Studying the scattering of N_2 off graphite at a range of incidence angles, Hase and co-workers found that scattering preferentially occurs close to the specular angle (but at slightly larger angles relative to the surface normal) and with fairly narrow angular distributions,[16] matching well the narrow scattering in the experiments here.

The wider polar angle distributions at lower incoming kinetic energies can also be observed in Figure 3, which shows the correlation between the polar angle and the final speed of
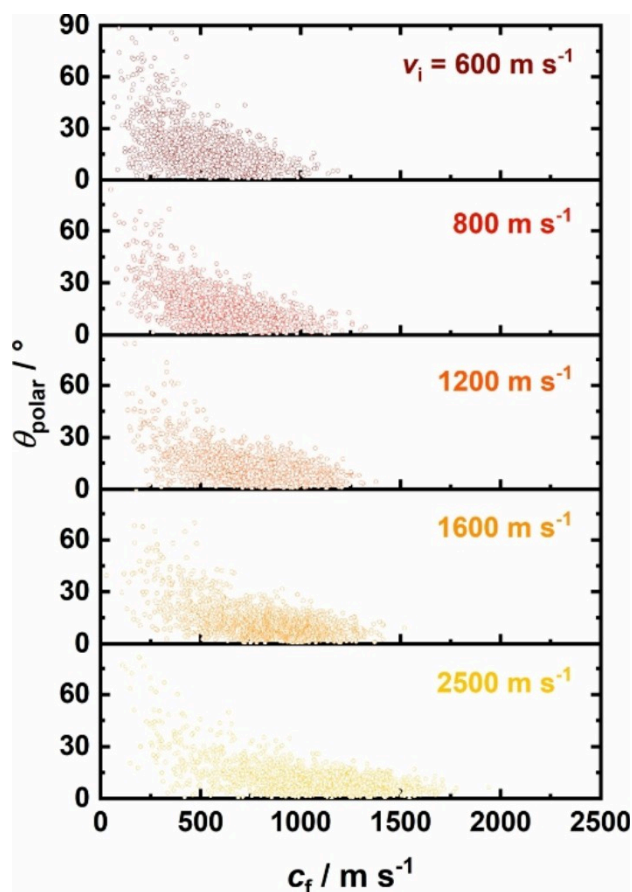
ChemPhysChem

Research Article
doi.org/10.1002/cphc.202200216

Chemistry
Europe
European Chemical
Societies Publishing

Figure 3. Polar angles θ_{polar} as a function of the final speed of the scattered NO molecules for the five different initial speeds as indicated.

Figure 4. Four different but characteristic trajectories of NO molecules scattering off graphene. Shown is the distance between the N atom (and *not* the center-of-mass of NO, in order to highlight rotational effects) and the average height of the six closest C atoms in graphene (not necessarily a hexagon) as a function of time. The 2500 m s^{-1} trajectory undergoes direct scattering, while the 600 m s^{-1} trajectory shows trapping-desorption behaviour. The two 1200 m s^{-1} trajectories (with the same initial slope) undergo direct scattering (yielding a rotationally excited NO) or permanent trapping (within the simulation time of 4 ps).

the scattered NO molecules (but – ignoring the y-axis – also shows the speed distribution and its shift towards speeds higher than the incoming speed which has already been better illustrated in Figure 1). The downward trend (or slope) for all incoming speeds shows that scattering along the surface normal retains the most kinetic energy, while more energy is lost to rotations or the graphene lattice vibrations when the NO scatters away from the surface normal.

There are several distinct scattering mechanisms when the NO interacts with the graphene surface which largely depend on the incoming velocity, with some examples being shown in Figure 4. Previous studies have demonstrated that NO scatters off (a number of different) surfaces via two different mechanisms, namely an inelastic component which dominates at high incidence energies, and a trapping-desorption mechanism which dominates at low incidence energies and glancing angles.[21,23,24] A typical result of the NO scattering with higher initial velocities is a single 'bounce' off the graphene surface with very little rotation of the NO molecule itself, resulting in the almost straight yellow line in Figure 4 for an initial velocity of 2500 m s^{-1}. At lower initial velocities, a higher likelihood of trapping on the graphene surface can be observed, either 1) trapping for a short time, during which the NO bounces several times on the surface before being released into the vacuum as
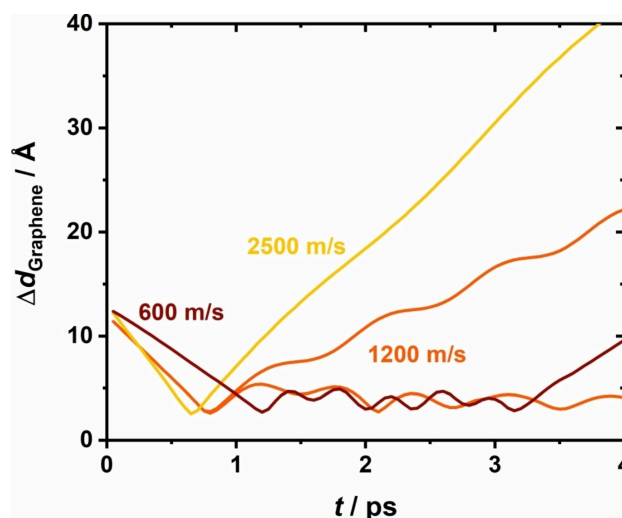
is the case for the 600 m s^{-1} initial velocity trajectory, or 2) the NO can be trapped for the entire simulation duration (4 ps) as shown for the second 1200 m s^{-1} trajectory. Previous work also displayed these three scattering pathways although using longer simulation times of 10 ps and 25 ps.[15–17] Evidence from experimental work suggests that the majority of those molecules which are 'trapped' at the end of a simulation run do eventually leave the surface (at adsorption energies a fraction of the thermal energy, residence times are likely to be short) and do *not* thermalize at the surface.[15] Theoretical work involving O$_2$ scattering off graphite demonstrated that around 60 % of the molecules scattered with just a single bounce and a further 20 % underwent multiple bounces.[17]

Permanent trapping of NO at the surface is more likely to occur at lower initial velocities where there is less chance of the NO having sufficient energy to overcome the attractive van der Waals (vdW) forces after rebound, as shown in Figure 5. As is expected, the higher the initial velocity, the lower the chance of trapping. Interestingly, we also observe that for the five highest initial velocities, the rotationally excited molecules seem to have higher trapping probabilities (despite the initial kinetic energy of the NO molecules with and without rotational excitation being the same). A possible reason for this is that the rotating molecules are more likely to approach the graphene surface in a 'side-on' configuration, which would lead to a greater likelihood for the vdW forces to 'take a hold' of the NO. Another reason for this increased trapping could be that the rotating molecules are likely to scatter under a wider polar angle and hence spend more time close to the surface compared to NO molecules that scatter closer to the surface
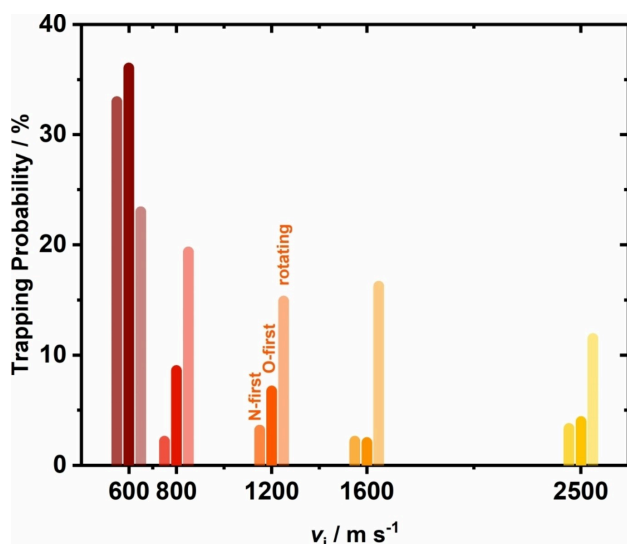
Figure 5. Trapping probabilities for collisions of NO molecules with graphene for the five indicated initial speeds, and separated for N-first and O-first orientation (without rotation), and NO molecules with a thermal rotational state distribution at 80 K.

Figure 6. Selected rotational state distributions of NO radicals scattered off graphene. Top-two panels for N-first and O-first orientation without initial rotational excitation, bottom-two panels for initial thermal 80 K rotational distributions. Open symbols for 600, 800, and 1200 m s^{-1}, closed symbols for 1600 and 2500 m s^{-1}.

normal, again increasing the likelihood of vdW interactions between the graphene surface and the NO to trap the nitric oxide. Previous work has shown that trapping increases in likelihood as the incidence angle increases,[15] this suggests the increased trapping at lower velocities and in case of rotating molecules are indeed due to the vdW interactions as these effects would be felt more strongly at larger incidence angles. Research at even longer timescales (25 ps) also shows trapping probabilities increasing at lower velocities and higher incidence angles.[16]

The final rotational state distributions after scattering off the graphene surface shown in Figure 6 reveal two findings. Firstly, the faster initial velocities result in higher rotational energy levels being populated, i.e. translational motion is coupled to rotational motion. Secondly, the initially rotationally excited molecules also have a higher rotational energy after collisions. Research by Hase and co-workers suggest that energy transfer is slightly dependent on incident velocity with a slightly higher proportion of energy going into rotations at lower velocities.[16] If we focus on the 1600 m s^{-1} and 2500 m s^{-1} trajectories for the rotating NO molecules, there appears to be evidence for rotational rainbows, most interestingly in the case for the 2500 m s^{-1} which looks to display a 'double rainbow'. Rotational rainbows from NO scattering have been observed experimentally in both the gas phase[27] and from solid surfaces.[28] Theoretical studies have shown the presence of rotational rainbows off graphite, though only at high surface temperatures.[18,19] Seminal studies on the scattering of NO off Ag(111) have also found evidence for rotational rainbows.[29,30] Later studies involving NO on Ag(111) concluded that the orientation of the incoming molecule has an effect on the prominence of rotational rainbows, perhaps explaining why the rainbows are better seen in the simulations with rotating NO.[31]
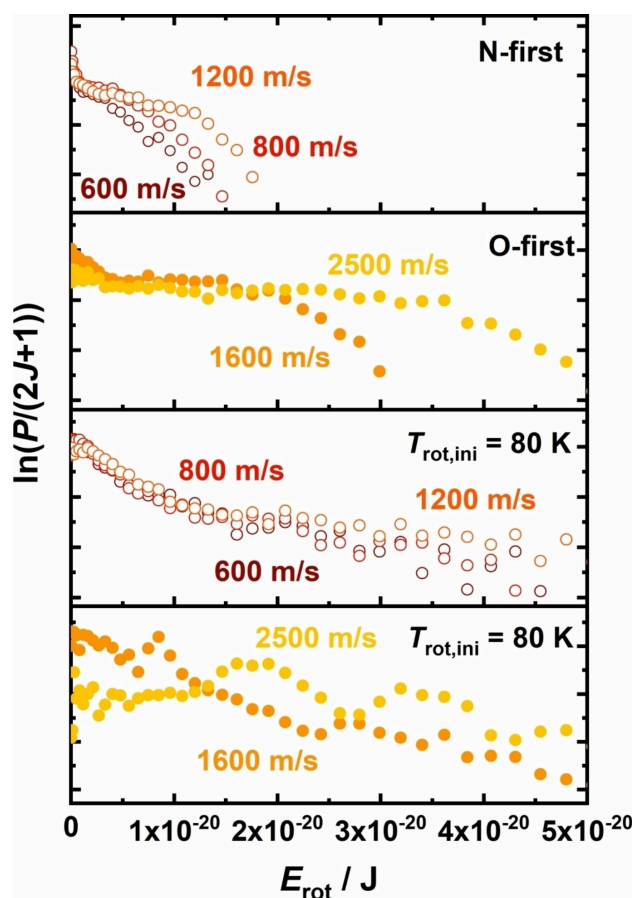
Studies of NO off graphite found that the NO is fully rotationally accommodated at surface temperatures below 170 K and scatters off with a rotational distribution that can be described by the surface temperature. Above 250 K, however, the NO is only partially accommodated and its rotational distribution can often not be described by a single temperature.[22,23] It was also found that in the case of NO off Ag(111) at low rotational levels ($J < 20$), a Boltzmann-like distribution can be observed, followed by higher populations again at higher J levels similar to our results shown in Figure 6, thus making it impossible to assign one single rotational temperature to the scattered NO molecules.

Figure 7 shows the height of the N atom in NO above the average of the six closest C atoms at the turning point of the NO (i.e. at the closest approach) as a function of the *final* velocity of that NO molecule. A clear inverse correlation can be seen between the shortest distance and the final velocity. Despite the graphene surface not being perfectly flat with shallow peaks and troughs due to surface phonons (leading to slight variations in the shortest distance), it can be assumed that this inverse correlation is due to those NO radicals which
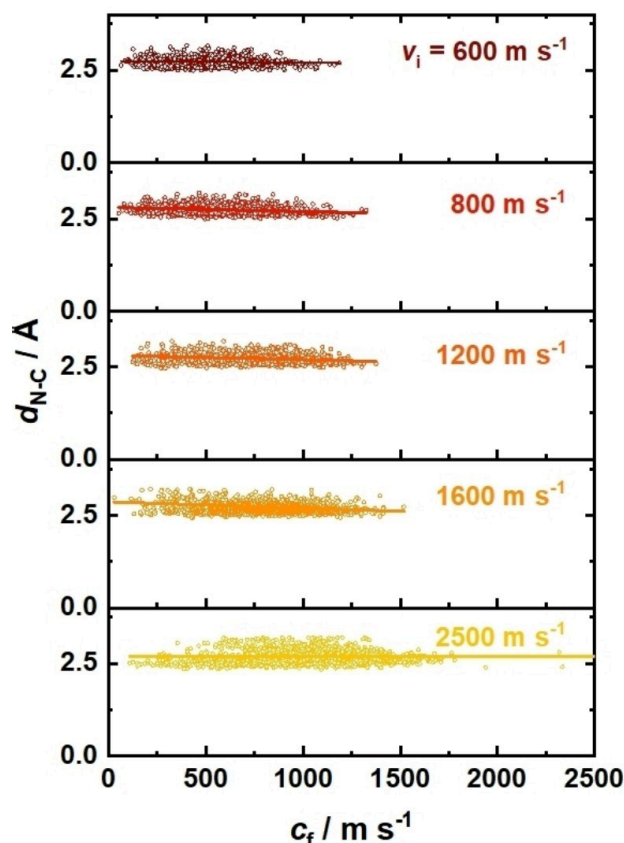
ChemPhysChem

Research Article
doi.org/10.1002/cphc.202200216

Chemistry Europe
European Chemical
Societies Publishing

Figure 7. Shortest distance between the N atom of NO and the average of six closest C atoms in graphene at the turning point as a function of final speed, with the linear fit only as a guide to the eye. All data for N-first orientation, but data is very similar for O-first orientation.

happen to get closer to the graphene surface experiencing a greater repulsive force, resulting in a faster scattering velocity.

Conclusions

In summary, NO scattering off graphene using MD simulations qualitatively agrees with the previous experiments in that the more energy the NO has initially, the higher the energy lost as a ratio of the total initial energy, i.e. a larger fraction of energy is lost to graphene. Separate modes can be seen once the NO collides with the graphene in both direct scattering which is dominant at higher incoming velocities, and trapping/multiple bounces dominating at lower incidence velocities. In terms of trapping probabilities, the likelihood of trapping greatly increased at lower incidence velocities but also for the rotating NO at each initial velocity, with the exception of 600 ms^{-1}. Narrow polar angle distributions were observed, with these

distributions becoming narrower as the initial velocity of the NO increased; those narrow angular distributions confirmed that we did not miss in our experimental work, in which we are not able to detect the whole 2π hemisphere above the surface, any contributions to the overall distribution. We detected a range of turning points for each of the five monoenergetic initial velocities, and these turning points correlate with the final velocity such that the closer the approach, the faster the final velocity. Two features stand out in the rotational distributions, namely 1) the translational energy of the NO is converted to rotational energy as seen by the fact that the higher the initial velocity, the higher the rotational energy levels populated, and 2) some evidence at higher incidence velocities for rotational rainbows. These simulations trigger us to perform further laboratory experiments at different initial velocities, which will also allow us to extract residence times at the surface.

Methodology

The molecular dynamics simulations described here were performed within the DL_POLY Classic suite using a combination of force fields.[32] A simulations box was selected with a 120° rhombus as a base in the x-y plane of length 17.3 Å each and a z dimension perpendicular to the x-y plane of length 45 Å. Periodic boundary conditions were applied along the x-y plane, but with no periodicity in the z dimension. The metal substrate was formed of a 6×6×6 array of gold atoms (with only the bottom layer being frozen in position, i.e. those Au atoms furthest away from the surface) whose interactions were described by a Gupta potential with parameters shown in Table 2.[33]

98 carbon atoms were positioned in a hexagonal 2D network in the x-y plane on top of the gold substrate. The bonds in the graphene sheet were described by a harmonic potential (rather than fixed bond lengths) to accurately reflect any compressions and stretches in the bonds as the NO collides with the graphene surface. A Morse bond potential as per equation 2 described the C—C bonds

$$V(r) = D[e^{-\alpha(r-r_0)} - 1]^2 \tag{2}$$

with parameters proposed by Kalosakas and co-workers,[34] using the accepted carbon-carbon internuclear distance in graphene of 1.42 Å, with $D = 5.7$ eV and $\alpha = 1.96$ Å^{-1}. This force field was selected as it has been derived from first principles, accurately describes the interactions in graphene and is suitable for atomistic simulations.

Angles and dihedrals were described by quartic and cosine functions, respectively, of the form (equations 3 and 4):

$$V_b(\theta) = \frac{k}{2}\left(\theta - \frac{2\pi}{3}\right)^2 - \frac{k'}{3}\left(\theta - \frac{2\pi}{3}\right)^3 \tag{3}$$

Table 2. Parameters used for the Gupta potential to describe interactions in gold.[33]													
λ	μ	α_∞[eV]	ζ	n_0	δ	β_∞[eV]	γ	Δ	η	R_∞[Å]	$\rho0$	ν	ξ
12.728	3.173	0.1730	6.5149	−1.234	1.593	2.7565	0.628	−2.041	1.952	2.927	0.144	6.247	3.330

ChemPhysChem

Research Article
doi.org/10.1002/cphc.202200216

**Chemistry
Europe**
European Chemical
Societies Publishing

$$V_t(\omega) = \frac{1}{2}V_2[1 - \cos(2\omega)] \tag{4}$$

where $k = 7.0$ eV rad^{-2} and $k' = 4.0$ eV rad^{-3}, and $V_2 = 0.23$ eV.[35]

Non-bonding interaction were described by Lennard-Jones 12–6 potentials of the form

$$U(r) = 4\varepsilon \left[\left(\frac{\sigma}{r} \right)^{12} - \left(\frac{\sigma}{r} \right)^6 \right] \tag{5}$$

with all parameters given by the universal force field set out by W. M. Skiff and co-workers,[36] with the exception of the gold and graphene interaction being developed by E. E. Helgee and A. Isacsson.[37] Respective values are provided in Table 3. We stress here that we have *not* benchmarked these potentials against ab initio calculations which would have likely yielded a much better potential,[16] and this possible discrepancy is one of the contributing factors for the only qualitative agreements between the simulations and experiments. Lorentz-Berthelot combining rules were applied for interactions between unlike atoms. The Lennard-Jones 12–6 potential was only applied to C–C interactions of carbon atoms at least four C–C bonds apart, i.e. not yet described by Morse bond potentials or angular or dihedral potentials.

The gold and graphene were relaxed and equilibrated by running simulations in an NVT ensemble regulated to 300 K by a Nosé-Hoover thermostat for 4 ns with a relaxation constant of 1 ps prior to the addition of a nitric oxide molecule. The equilibrated distance between the graphene and the top-layer of Au atoms is around 3 Å.

A single NO molecule was then positioned above the graphene surface, and its bond potential was also defined by a Morse potential with parameters $D_e = 6.61736$ eV, $\beta = 2.636$ Å^{-1} and $r_e = 1.151$ Å.[38] Placing such a single NO molecule in a randomly selected position in the x-y plane ~12 Å above the graphene is sufficient as interatomic forces were truncated after 7 Å. Both the N and O atom were then given a velocity of 600, 800, 1200, 1600, or 2500 m s^{-1} along the z axis towards the graphene (same geometry as in our experiments), i.e. no vibrational excitation was given to the NO molecule, just as no NO($v=1$) is expected in the cold molecular beam in our experiments. While these velocities do not match our experimental velocity exactly, they cover a range of velocities achievable in molecular beam experiments, and match our experimental kinetic energy to < 0.1 eV.

Three cases in terms of orientation and rotational excitation of the nitric oxide were investigated: 1) no rotational excitation, NO aligned along the surface normal with the N-oriented towards the surface (see Figure 1); 2) same as (1), but with O facing the surface; 3) with a rotational distribution representative of a thermal 80 K sample (roughly equivalent to a molecular beam) *in addition to* the translational energy, and a random orientation in space. 2000 trajectories were run for each orientation/rotational excitation case, with the NO originating from a different position within the x-y

plane for every run in each of those cases, giving 6000 trajectories in total for each of the five velocities, making a total of 30,000 trajectories.

The molecular dynamics simulations were run with a timestep of 1 fs for 4 ps (8 ps for 600 m s^{-1} simulations, all starting after the 4 ns equilibration of the graphene and gold). After the NO has interacted with the graphene, it was registered once traversing a virtual plane 8 Å above the graphene, where there is no longer any interaction between the graphene and the NO. Properties such as the positions and velocity components of both the N and O atoms in all three dimensions separately were recorded. Molecular speeds were extracted from center-of-mass shifts per unit time and binned in 20 m s^{-1} wide intervals. The simulation parameters are schematically shown in Figure 8.
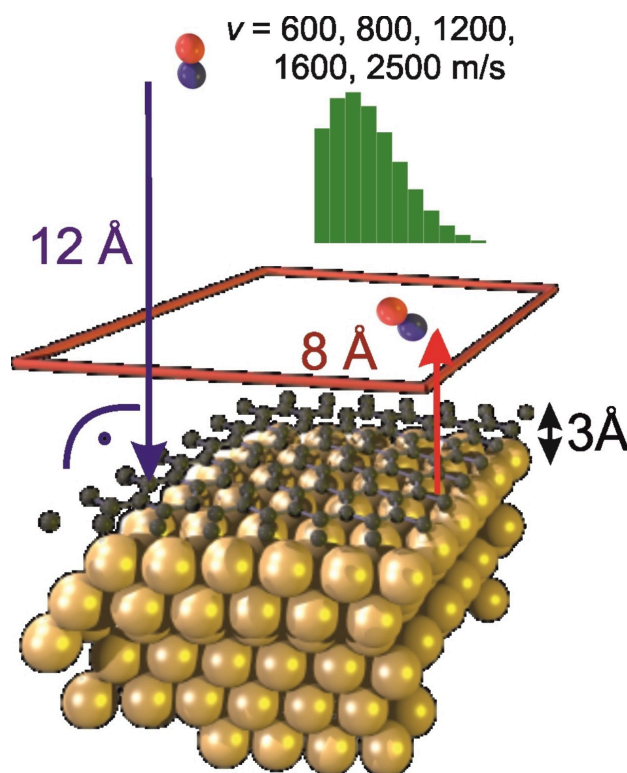
Figure 8. Schematic of input parameter of the molecular dynamics simulations. NO molecules are placed 12 Å above the graphene surface and given a certain velocity, and in some cases rotational excitation. They are directed along the surface normal towards a random position on the graphene, from where they scatter back before they are recorded when traversing a virtual plane 8 Å above the surface.

Table 3. Parameters for the van der Waals interactions.		
Interaction	ε [eV]	σ [Å]
C–C	0.004553	3.431
C–O	0.003442	3.2745
C–N	0.003691	3.346
N–Au	0.00225	3.0972
C–Au	0.0341	3.003
O–Au	0.002098	3.0259

Conflict of Interest

The authors declare no conflict of interest.

Data Availability Statement

The data that support the findings of this study are available from the corresponding author upon reasonable request.

[1] P. R. Arantes, A. Saha, G. Palermo, *ACS Cent. Sci.* **2020**, *6*, 1654.
[2] D. J. Tildesley, M. P. Allen, *Computer Simulation of Liquids*, Clarendon Press, Oxford, **1987**.
[3] C. Verma, H. Lgaz, D. K. Verma, E. E. Ebenso, I. Bahadur, M. A. Quraishi, *J. Mol. Liq.* **2018**, *260*, 99.
[4] E.-H. Patel, M. A. Williams, S. P. K. Koehler, *J. Phys. Chem. B* **2017**, *121*, 233.
[5] J. N. Murrell, S. D. Bosana, *Chem. Soc. Rev.* **1992**, *21*, 17.
[6] A. Monari, J.-L. Rivail, X. Assfeld, *Acc. Chem. Res.* **2013**, *46*, 596.
[7] T. V. Albu, J. C. Corchado, D. G. Truhlar, *J. Phys. Chem. A* **2001**, *105*, 8465.
[8] T. D. Kühne, *Wiley Interdiscip. Rev. Comput. Mol. Sci.* **2014**, *4*, 391.
[9] T. Greenwood, S. P. K. Koehler, *J. Phys. Chem. C* **2021**, *125*, 17853.
[10] R. Nieman, A. J. A. Aquino, H Lischka, *J. Phys. Chem. A* **2021**, *125*, 1152.
[11] H. Y. Jiang, M. Kammler, F. Z. Ding, Y. Dorenkamp, F. R. Manby, A. M. Wodtke, T. F. Miller, A. Kandratsenka, O. Bünermann, *Science* **2019**, *364*, 379.
[12] H. Jiang, X. Tao, M. Kammler, F. Ding, A. M. Wodtke, A. Kandratsenka, T. F. Miller III, O. Bünermann, *J. Phys. Chem. Lett.* **2021**, *12*, 1991.
[13] R. Nieman, R. Spezia, B. Jayee, T. K. Minton, W. L. Hase, H. Guo, *J. Chem. Phys.* **2020**, *153*, 184702.
[14] B. Jayee, R. Nieman, T. K. Minton, W. L. Hase, H. Guo, *J. Phys. Chem. C* **2021**, *125*, 9795.
[15] N. A. Mehta, V. J. Murray, C. Xu, D. A. Levin, T. K. Minton, *J. Phys. Chem. C* **2018**, *122*, 9859.
[16] M. Majumder, H. N. Bhandari, S. Pratihar, W. L. Hase, *J. Phys. Chem. C* **2018**, *122*, 612.
[17] A. R. Santamaría, M. Alducin, R. D. Muiño, J. I. Juaristi, *J. Phys. Chem. C* **2019**, *123*, 31094.
[18] J. B. C. Pettersson, G. Nyman, L. Holmlid, *J. Chem. Phys.* **1988**, *89*, 6963.
[19] G. Nyman, L. Holmlid, J. B. C. Pettersson, *J. Chem. Phys.* **1990**, *93*, 845.
[20] J. Oh, T. Kondo, K. Arakawa, Y. Saito, W. W. Hayes, J. R. Manson, J. Nakamura, *J. Phys. Chem. A* **2011**, *115*, 7089.
[21] J. A. Barker, D. J. Auerbach, *Surf. Sci. Rep.* **1984**, *4*, 1.
[22] M. C. Lin, G. Ertl, *Annu. Rev. Phys. Chem.* **1986**, *37*, 587.
[23] J. Häger, M. Fink, H. Walther, *Surf. Sci.* **2004**, *550*, 35.
[24] F. Frenkel, J. Häger, W. Krieger, H. Walther, G. Ertl, J. Segner, W. Vielhaber, *Chem. Phys. Lett.* **1982**, *90*, 225.
[25] C. T. Rettner, E. K. Schweizer, C. B. Mullins, *J. Chem. Phys.* **1989**, *90*, 3800.
[26] A. Rodríguez-Fernández, L. Bonnet, C. Crespos, P. Larrégaray, R. Díez Muiño, *J. Phys. Chem. Lett.* **2019**, *10*, 7629.
[27] X. D. Wang, P. A. Robertson, F. J. J. Cascarini, M. S. Quinn, J. W. McManus, A. J. Orr-Ewing, *J. Phys. Chem. A* **2019**, *123*, 7758.
[28] A. E. Wiskerke, C. A. Taatjes, A. W. Kleyn, R. J. W. E. Lahaye, S. Stolte, D. K. Bronnikov, B. E. Hayden, *Faraday Discuss.* **1993**, *96*, 297.
[29] A. W. Kleyn, A. C. Luntz, D. J. Auerbach, *Surf. Sci.* **1982**, *117*, 33.
[30] A. W. Kleyn, A. C. Luntz, D. J. Auerbach, *Phys. Rev. Lett.* **1981**, *47*, 1169.
[31] A. W. Kleyn, *Surf. Rev. Lett.* **1994**, *1*, 157.
[32] I. T. Todorov, W. Smith, K. Trachenko, M. T. Dove, *J. Mater. Chem.* **2006**, *16*, 1911.
[33] J. T. Titantah, M. Karttunen, *Eur. Phys. J. B* **2013**, *86*, 1.
[34] G. Kalosakas, N. N. Lathiotakis, C. Galiotis, K. Papagelis, *J. Appl. Phys.* **2013**, *113*, 134307.
[35] Z. G. Fthenakis, G. Kalosakas, G. D. Chatzidakis, C. Galiotis, K. Papagelis, N. N. Lathiotakis, *Phys. Chem. Chem. Phys.* **2017**, *19*, 30925.
[36] A. K. Rappe, C. J. Casewit, K. S. Colwell, W. A. Goddard, W. M. Skiff Uff, *J. Am. Chem. Soc.* **1992**, *114*, 10024.
[37] E. E. Helgee, A. Isacsson, *AIP Adv.* **2016**, *6*, 015210.
[38] S. Mishra, M. Meuwly, *Biophys. J.* **2009**, *96*, 2105.